New Analytical Study of Non-Newtonian Jeffery Hamel Flow of Casson Fluid in Divergent and Convergent Channels by Perturbation Iteration Algorithm

Abeer Majeed Jasim*, Ali Juwaid Al-Maliki

Department of Mathematics, College of Sciences, University of Basrah, Basra. Iraq

*Corresponding author: E-mail: abeer.jassem@yahoo.com

Doi:10.29072/basjs.202113

Abstract

Perturbation iteration algorithm (PIA) is used to solve Jeffery Hamel flow problem of non-Newtonian fluid which is Casson fluid (JHFCF) to simplify a suitable transformation of similarities that applied to obtain a non- linear ordinary differential equation. The resulting equation is solved by PIA and numerically using fourth order Runge Kutta (RK4). Both solutions are compared by the variance of the parameter method (VPM) in order to check the efficacy of the provided (PIA) approach. For both diverging and converging channels, the influences of the parameters are demonstrated by graphical simulation.

Article inf.

Received: 2/03/2021

Accepted 25/3/2021

Published 1/04/2021

Keywords:

Perturbation Iteration Algorithm, Solution Series, Jeffery Hamel Flow, Casson Fluid, Analysis of Convergence.

1. Introduction:

The flow through tapered walls has gained a lot of interest because of its wide range of applications in the aerospace, chemical, civil, environmental, bio- mechanical engineering, and mechanical. The blood is considered as a kind of flow in the human body where capillaries and arteries are linked to each other. In addition, these applications are also related in to the flow in channels and rivers. A mathematical model of the flows through non parallel walls was firstly introduced by Jeffrey[1] and Hamel [2]. These types of flows are known as the Jeffery Hamel flows of Casson fluid problem. Extensively, JHFCFP has been discussed by several authors in many types of research [3–7]. Because of the complex rheological nature of non-Newtonian fluids, there is no single model that can be used to simulate the whole class. Therefore, many non-Newtonian flow models have been presented over the years. Casson fluid is one of these models that exhibit blood type behavior [8, 9]. Inherently, most of the models that describing a physical problem are accomplished in the form of non- linearity. Therefore, the exact solution is not found, furthermore approximation techniques are developed to solve these complex problems including several analytical methods such as domain decomposition method (ADM), variance of the parameter method (VPM) and perturbation iteration algorithm(PIA) [10–15]. The objective of this paper is the search for analytical approximate solution for the Non-linear problem which describes incompressible viscous Jeffery Hamel flow of Casson Fluid. In addition, we studies PIA is based on algorithm which are classified with respect to the number of terms in the perturbation expansion n1 and the degrees of derivatives in the Taylor expansions n_2. However, this method has been named as PIA $(n_1, n_2), n_1, n_2$ = 1,2,…. P IA (n1,) have a famous technique for solving problems in different fields of science and engineeringn_2 In this study, PIA is used to solve a rather complex problem JHFP in diverging and converging channels to find analytical approximate solution and known the effect of physical parameters on these solutions. The main advantage of this method is that, it reduces the computational work while still maintaining a higher level of accuracy. In addition, PIA (1,1) is analyze to give the sufficient conditions for convergence of the approximation series solution generated by PIA.

2. Perturbation Iteration Algorithm

Perturbation Iteration techniques are a class of analytical methods and important for determining approximate solutions of nonlinear algebraic equations, differential equations and integral-differential equations. They are useful for demonstrating, predicting, and describing phenomena in vibrating systems that are caused by nonlinear effects. In mathematics, perturbation methods comprise mathematical methods for finding an approximate solution to a problem, by starting from the exact solution of a related simpler problem. Perturbation is widely used when the problem at hand does not have a known exact solution, but can be expressed as a small change to a known solvable problem. Perturbation methods is used in a wide range of Physical fields. To explain the idea of Perturbation Iteration Algorithm(1,1), consider the nonlinear ordinary differential equation as form [22]:

$$D\left(\eta,\ \Psi(\eta),\ \frac{d\Psi}{d\eta},\ \frac{d^2\Psi}{d\eta^2},\frac{d^3\Psi}{d\eta^3},\dots,\ \frac{d^{(n-1)}\Psi}{d\eta^{(n-1)}},\ \frac{d^{(n)}\Psi}{d\eta^{(n)}}\right)=0, \tag{1}$$

where D is a function of Ψ and its drivatives, Ψ is an unkown function and denote η spactial dependent variable. In Equation (1), we can add auxiliary perturbation parameter ε as shown in the following equation:

$$D\left(\eta,\ \Psi(\eta),\ \frac{d\Psi}{d\eta},\ \frac{d^2\Psi}{d\eta^2},\frac{d^3\Psi}{d\eta^3},\dots,\ \frac{d^{(n-1)}\Psi}{d\eta^{(n-1)}},\ \frac{d^{(n)}\Psi}{d\eta^{(n)}}\right)=0, \tag{2}$$

rewriting the Equation (1) as the following;

$$D\left(\eta,\Psi_{m+1},\ \frac{d\Psi_{m+1}}{d\eta},\ \frac{d^2\Psi_{m+1}}{d\eta^2},\dots,\ \frac{d^{(n-1)}\Psi_{m+1}}{d\eta^{(n-1)}},\ \frac{d^{(n)}\Psi_{m+1}}{d\eta^{(n)}},\varepsilon\right)=0, \tag{3}$$

where, m represents the mth iteration with defined perturbation expansions with correction term as follow;

$$\Psi_1=\Psi_0+\varepsilon(\Psi_c)_{0,}$$

$$\Psi_2=\Psi_1+\varepsilon(\Psi_c)_{1,}$$

$$\Psi_3=\Psi_2+\varepsilon(\Psi_c)_{2,}$$

$$\vdots$$

$$\Psi_{m+1}=\Psi_m+\varepsilon(\Psi_c)_m\,, \tag{4}$$

where, ε is a small perturbation parameter and Ψ_c is the correction term in the perturbation expansion. Now Substituting (4) in (3), we obtain

$$D(\Psi_m(\varepsilon)+\varepsilon(\Psi_c)_m,\Psi'_m(\eta)+\varepsilon(\Psi_c)'_m,\Psi''_m(\eta)+\varepsilon(\Psi_c)''_m,\Psi'''_m(\eta)+\varepsilon(\Psi_c)'''_m,\dots,\Psi_m^{n-1}(\eta)+\varepsilon(\Psi_c)_m^{n-1},\ \Psi_m^n(\eta)+\varepsilon(\Psi_c)_m^n,\ \varepsilon)=0, \quad (5)$$

in the next step we take the Taylor series expansion for the first order derivative in the neighborhood of $\varepsilon=0$, yields

$$D\left(\eta,\Psi_{m+1}(\eta),\ \frac{d\Psi_{m+1}}{d\eta},\frac{d^2\Psi_{m+1}}{d\eta^2},\dots,\frac{d^{(n-1)}\Psi_{m+1}}{d\eta^{(n-1)}},\frac{d^{(n)}\Psi_{m+1}}{d\eta^{(n)}},\varepsilon\right)+\varepsilon\frac{dD}{d\Psi_m}.(\Psi_c)_m\Big|_{\varepsilon=0}+$$

$$\varepsilon\frac{dD}{d\Psi'_m}.(\Psi_c)'_m\Big|_{\varepsilon=0}+\cdots+\varepsilon\frac{dD}{d\Psi_m^{(n-1)}}.(\Psi_c)_m^{(n-1)}\Big|_{\varepsilon=0}+\varepsilon\frac{dD}{d\Psi_m^{(n)}}.(\Psi_c)_m^{(n)}\Big|_{\varepsilon=0}+\varepsilon\frac{dD}{d\varepsilon}=0, \quad (6)$$

rearranging Equation (6) gives

$$(\Psi_c)_m^{(n)}=-\frac{-D}{\varepsilon\frac{dD}{d\Psi_m^{(n)}}}-\frac{\frac{dD}{d\Psi_m}}{\frac{dD}{d\Psi_m^{(n)}}}.(\Psi_c)_m-\frac{\frac{dD}{d\Psi'_m}}{\frac{dD}{d\Psi_m^{(n)}}}.(\Psi_c)'_m-\cdots-\frac{\frac{dD}{d\Psi_m^{(n-1)}}}{\frac{dD}{d\Psi_m^{(n)}}}.(\Psi_c)_m^{(n-1)}-\frac{\frac{dD}{d\varepsilon}}{\frac{dD}{d\Psi_m^{(n)}}}. \quad (7)$$

Now, all calculations in Equation (7) are performed at $\varepsilon=0$, results in Equation (7) get ordinary differential equation. This ordinary differential equation is solved to obtain $(\Psi_c)_m(\eta)$. In order to find the first correction term, Ψ_0 is a trial function satisfying the initial condition. Substituting Ψ_0 into Eq. (7), the first order problem is:

$$(\Psi_c)_0^{(n)}=-\frac{-D}{\varepsilon\frac{dD}{d\Psi_0^{(n)}}}-\frac{\frac{dD}{d\Psi_0}}{\frac{dD}{d\Psi_0^{(n)}}}.(\Psi_c)_0-\frac{\frac{dD}{d\Psi'_0}}{\frac{dD}{d\Psi_0^{(n)}}}.(\Psi_c)'_0-\cdots-\frac{\frac{dD}{d\Psi_0^{(n-1)}}}{\frac{dD}{d\Psi_0^{(n)}}}.(\Psi_c)_0^{(n-1)}-\frac{\frac{dD}{d\varepsilon}}{\frac{dD}{d\Psi_0^{(n)}}}, \quad (8)$$

thus, we can express the approximate solutions in the following way, firstly can be defined:

$$\Psi_0=C_0,\ (\Psi_c)_m=C_{m+1}, \quad (9)$$

and the other solutions can be defined in the following iterations

$$\Psi_0=C_0,$$
$$\Psi_1=\Psi_0+(\Psi_c)_0=C_0+C_1,$$
$$\Psi_2=\Psi_1+(\Psi_c)_1=C_0+C_1+C_2,$$
$$\vdots$$
$$\Psi_{m+1}=\Psi_n+(\Psi_c)_m=C_0+C_1+C_2+\cdots+C_{m+1}=\sum_{i=0}^{m+1}C_i. \quad (10)$$

Consequently, the value of $(\Psi_c)_{m+1}$ are substituted in Equation (4) to obtain on $\Psi_m(\eta)$. It is the approximate-analytical solution required, which is in the form of the power series. The solution of Equation (2) can be represented as:

$$\Psi(\eta)=\lim_{n\to\infty}\Psi_{m+1}=\sum_{i=0}^{\infty}C_i.$$

3. Mathematical Formulation

Consider the flow of a Casson fluid initiated due to source or sink at the intersection of two rigid plane walls. The angle between the walls is taken as 2κ The flow is assumed to be symmetric and purely radial $u_{\dot{r}}$ as shown in Figure (1). The model of fluid flow composed of the continuity equation describing conservation of mass, momentum equation derived from Newton second law. These equations are defined mathematically as follows [15] :

$$\nabla . \ U = 0 \ , \tag{11}$$

$$\rho \left[\frac{\partial U}{\partial t} + (U.\nabla U) \right] = \ -\nabla p + \nabla \tau_{ij}. \tag{12}$$

Such that U is the fluid velocity, ∇ is the derivative operator *(gradient)*, ρ is the fluid density, and p is the hydrodynamic pressure. The following equation shows the viscosity of the liquid [11]

$$\tau_{ij} = 2\left(\mu_B + \frac{p_y}{\sqrt{2\pi}}\right) c_{ij}, \quad \pi \neq \pi_c, \tag{13}$$

where $\pi = c_{ij}c_{ij}$ with c_{ij} being the (i , j) the components of the deformation rate, π_c is the product of the deformation rate with itself, π_c denotes a critical value of this product based on a non-Newtonian model, μ_B denotes the plastic dynamic viscosity of non-Newtonian fluids and p_y is the yield stress of the fluid. These assumptions mean that the velocity field is of the type $U = \left[u_{\dot{r}}(\dot{r}, \dot{\theta}\ ), 0, 0\right]$. The equations of continuity and momentum for this problem are:

$$\frac{\partial u_{\dot{r}}(\dot{r},\dot{\theta})}{\partial \dot{r}} + \frac{1}{r} u_{\dot{r}}(\dot{r},\dot{\theta}) = 0, \tag{14}$$

$$-u_{\dot{r}}(\dot{r},\dot{\theta}) \frac{\partial u_{\dot{r}}(\dot{r},\dot{\theta})}{\partial \dot{r}} - \frac{1}{\rho} \ \frac{\partial p}{\partial \dot{r}} + \nu \left(1 + \frac{1}{\beta}\right) \left[\frac{\partial^2 u_{\dot{r}}(\dot{r},\dot{\theta})}{\partial r^2} + \frac{1}{\dot{r}} \ \frac{\partial u_{\dot{r}}(\dot{r},\dot{\theta})}{\partial \dot{r}} + \frac{1}{\dot{r}^2} \frac{\partial^2 u_{\dot{r}}(\dot{r},\dot{\theta})}{\partial \theta^2} - \frac{u_{\dot{r}}(\dot{r},\dot{\theta})}{\dot{r}^2} \right] = 0, \tag{15}$$

$$-\frac{1}{\rho \dot{r}} \frac{\partial \mathrm{P}}{\partial \theta} + \frac{2\mathrm{v}}{\dot{r}^2} \left(1 + \frac{1}{\beta}\right) \frac{\partial u_{\dot{r}}(\dot{r},\dot{\theta})}{\partial \theta} = 0, \tag{16}$$

the auxiliary conditions of the problem JHFCF are

$$u_{\dot{r}} = U_{\dot{r}}, \quad \frac{\partial u_{\dot{r}}}{\partial \theta} = 0 \quad at \quad \dot{\theta} = 0,$$

$$u_{\dot{r}} = 0, \quad \text{at} \quad \dot{\theta} = \kappa, \tag{17}$$

where $\nu = \frac{\mu_B}{\rho}$ is kinematic viscosity, p is the pressure, and $U_{\dot{r}}$ is the veloctity at the center line of the channel at $\dot{r} = 0$. To remove the value of pressure p, the derivation of Equations (15) and (16) with respect to $\dot{\theta}$, $\dot{r}$ respectively as:

$$-\frac{\partial^2 u_{\dot{r}}}{\partial \dot{\theta}\, \partial \dot{r}} - u_{\dot{r}} \frac{\partial^2 u_{\dot{r}}}{\partial \dot{\theta}\, \partial \dot{r}} - \frac{1}{\rho} \frac{\partial^2 p}{\partial \dot{\theta}\, \partial \dot{r}} + \nu \left(1 + \frac{1}{\beta}\right) \left[\frac{\partial^3 u_{\dot{r}}}{\partial \dot{\theta} \partial \dot{r}^2} + \frac{1}{\dot{r}} \frac{\partial^2 u_{\dot{r}}}{\partial \dot{\theta} \partial \dot{r}} + \frac{1}{\dot{r}^2} \frac{\partial^3 u_{\dot{r}}}{\partial \dot{\theta}^3} - \frac{1}{\dot{r}^2} \frac{\partial u_{\dot{r}}}{\partial \dot{\theta}} \right] = 0, \tag{18}$$

$$-\frac{1}{\rho}\frac{\partial^2 \mathrm{P}}{\partial\dot{\theta}\,\partial\dot{r}}+\frac{1}{\rho\dot{r}}\frac{\partial \mathrm{P}}{\partial\dot{\theta}}+\nu\left(1+\frac{1}{\beta}\right)\left[\frac{2}{\dot{r}}\frac{\partial^2 u_{\dot{r}}}{\partial\dot{\theta}\,\partial\dot{r}}-\frac{4}{\dot{r}^2}\frac{\partial u_{\dot{r}}}{\partial\dot{\theta}}\right]=0, \tag{19}$$

now by subtracting the two equations (18) from (19) we get

$$-\frac{\partial^2 u_{\dot{r}}}{\partial\dot{\theta}\,\partial\dot{r}}-u_{\dot{r}}\frac{\partial^2 u_{\dot{r}}}{\partial\dot{\theta}\,\partial\dot{r}}-\frac{1}{\rho\dot{r}}\frac{\partial P}{\partial\dot{\theta}}+\nu\left(1+\frac{1}{\beta}\right)\left[\frac{\partial^3 u_{\dot{r}}}{\partial\dot{\theta}\partial\dot{r}^2}-\frac{1}{\dot{r}}\frac{\partial^2 u_{\dot{r}}}{\partial\dot{\theta}\partial\dot{r}}+\frac{1}{\dot{r}^2}\frac{\partial^3 u_{\dot{r}}}{\partial\dot{\theta}^3}+\frac{3}{\dot{r}^2}\frac{\partial u_{\dot{r}}}{\partial\dot{\theta}}\right]=0, \tag{20}$$

by integrating both sides with respect to $\dot{r}$ for continuity equation (14) in the form

$$f(\dot{\theta})=\dot{r}u_{\dot{r}}(\dot{r},\dot{\theta}), \tag{21}$$

the dimensionless variables with the Equation (21), can make the problem dimensionless,

$$\Psi(\eta)=\frac{f(\theta)}{\dot{r}U_{\dot{r}}},\qquad \gamma=\dot{r}U_{\dot{r}},\qquad \eta=\frac{\dot{\theta}}{\kappa},\qquad u_{\dot{r}}(\dot{r},\dot{\theta})=\frac{\gamma}{\dot{r}}\,\Psi(\eta). \tag{22}$$

From Equation (22), we find the required derivatives

$$\frac{\partial \mathrm{u}_{\dot{\mathrm{r}}}}{\partial\theta}=\frac{\gamma}{\dot{\mathrm{r}}\kappa}\frac{\mathrm{d}\Psi(\eta)}{\mathrm{d}\eta},\qquad \frac{\partial^3 \mathrm{u}_{\dot{\mathrm{r}}}}{\partial\theta^3}=\frac{\gamma}{\kappa^3\dot{\mathrm{r}}}\frac{\mathrm{d}^3\Psi(\eta)}{\mathrm{d}\eta^3},\qquad \frac{\partial^3 \mathrm{u}_{\dot{\mathrm{r}}}}{\partial \mathrm{r}^2\,\partial\theta}=\frac{2\gamma}{\kappa\dot{\mathrm{r}}^3}\frac{\mathrm{d}\Psi(\eta)}{\mathrm{d}\eta},$$

$$\frac{\partial \mathrm{u}_{\dot{\mathrm{r}}}}{\partial \mathrm{r}}=\frac{-\gamma}{\dot{\mathrm{r}}^2}\Psi(\eta),\qquad \frac{\partial^2 \mathrm{u}_{\dot{\mathrm{r}}}}{\partial\dot{\mathrm{r}}\,\partial\theta}=\frac{-\gamma}{\kappa\dot{\mathrm{r}}^2}\frac{\mathrm{d}\Psi(\eta)}{\mathrm{d}\eta},\qquad \frac{\partial^2 \mathrm{u}_{\dot{\mathrm{r}}}}{\partial\dot{\mathrm{r}}^2}=\frac{2\gamma}{\dot{\mathrm{r}}^3}\Psi(\eta), \tag{23}$$

now, from equation (20) and substituting the above derivative into the Equation (23) yield

$$-\frac{2\gamma^2}{\kappa\dot{r}^3}\Psi(\eta)\frac{d\Psi(\eta)}{d\eta}-\nu\left(1+\frac{1}{\beta}\right)\left[\frac{\gamma}{\kappa^3\dot{r}^3}\frac{d^3\Psi(\eta)}{d\eta^3}+\frac{4\gamma}{\kappa\dot{r}^3}\frac{d\Psi(\eta)}{d\eta}\right]=0, \tag{24}$$

after simplify the Equation (24) , we get

$$\left(1+\frac{1}{\beta}\right)\frac{d^3\Psi(\eta)}{d\eta^3}+2\kappa R_e\Psi(\eta)\frac{d\Psi(\eta)}{d\eta}+4\kappa^2\left(1+\frac{1}{\beta}\right)\frac{d\Psi(\eta)}{d\eta}(\eta)=0. \tag{25}$$

The boundary condition of the problem dimensionless are

$$\Psi(0)=1,\qquad \frac{\mathrm{d}\Psi(0)}{\mathrm{d}\eta}=0,\qquad \Psi(1)=0. \tag{26}$$

$R_e=\frac{\dot{r}U_{\dot{r}}\,\kappa}{\nu}$ is Reynolds number, can classified to two cases as:

- Divergent Channel : $\kappa>0$, $U_{\dot{r}}>0$,
- Convergent Channel : $\kappa<0$, $U_{\dot{r}}<0$,

the values of the skin friction coefficient can be obtained by using

$$C_\Psi=\frac{\tau_{\dot{r}\dot{\theta}}}{U_{\dot{r}}^2}\bigg|_{\eta=1}=\frac{1}{R_e}\left(1+\frac{1}{\beta}\right)\frac{d\Psi(1)}{d\eta}, \tag{27}$$

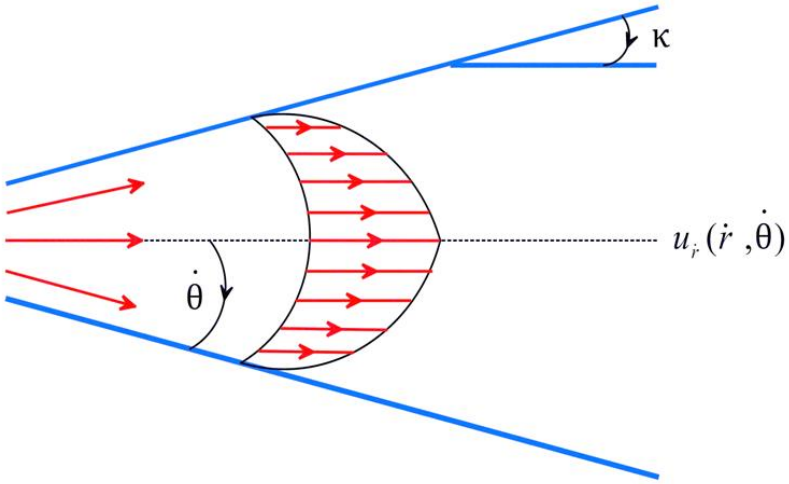

Figure 1 : Model diagram of Jeffery Hamel Flow of Casson fluid

4.Application of the Jeffery-Hamel Flow Problem.

The application of the PIA(1,1) by the steps of its algorithm to the nonlinear differential Equation in order to find an analytical approximate solution, can be illustrated as follows;

$$\left(1+\frac{1}{\beta}\right)\frac{d^3\Psi(\eta)}{d\eta^3}+2\kappa R_e\,\Psi(\eta)\frac{d\Psi(\eta)}{d\eta}+4\kappa^2\left(1+\frac{1}{\beta}\right)\frac{d\Psi(\eta)}{d\eta}=0, \tag{28}$$

subject boundary condition are:

$$\Psi(0)=1\,,\ \frac{d\Psi(0)}{d\eta}=0,\qquad \Psi(1)=0, \tag{29}$$

the problem of the auxiliary perturbation parameter ε are

$$D\left(\Psi(\eta),\frac{d\Psi(\eta)}{d\eta},\frac{d^3\Psi(\eta)}{d\eta^3},\varepsilon\right)=\left(1+\frac{1}{\beta}\right)\frac{d^3\Psi(\eta)}{d\eta^3}+2\varepsilon\kappa R_e\,\Psi(\eta)\frac{d\Psi(\eta)}{d\eta}+4\varepsilon\kappa^2\left(1+\frac{1}{\beta}\right)\frac{d\Psi(\eta)}{d\eta}, \tag{30}$$

perturbation expansions with only one corrections term are given as follows:

$$\Psi_{n+1}=\Psi_n+\varepsilon(\Psi_C)_n, \tag{31}$$

substituting Equation (31) into Equation (30), Taylor series with first order derivative terms about $\varepsilon=0$, yields

$$D(\Psi_n,\Psi_n',,\Psi_n'',\Psi_n''',0)+\varepsilon[\,D_{\Psi_n}(\Psi_C)_n+D_{\Psi'_n}(\Psi_C)'_n+D_{\Psi'''_n}(\Psi_C)'''_n+D_\varepsilon]=0, \tag{32}$$

now, we apply Equation (30) to Equation (32) and we get the following derivatives:

$$D_{\Psi_n} = 2\varepsilon\kappa R_e \Psi_n',$$
$$D_{\Psi'_n} = 2\varepsilon\kappa R_e \Psi_n + 4\varepsilon\kappa^2\left(1+\frac{1}{\beta}\right),$$
$$D_{\Psi'''_n} = \left(1+\frac{1}{\beta}\right), \quad (33)$$
$$D(\Psi_n, \Psi_n', \Psi_n''', 0) = \left(1+\frac{1}{\beta}\right)\Psi_n''',$$
$$D_\varepsilon = 2\kappa R_e \Psi_n \Psi_n' + 4\kappa^2\left(1+\frac{1}{\beta}\right)\Psi_n',$$

by calculating all derivatives at $\varepsilon = 0$ and substituting the results into (32) yields the following linear ordinary differential equations

$$(\Psi_c)_n''' = -\frac{1}{\varepsilon}\Psi_n'''(\eta) - 2\left(\frac{\beta}{\beta+1}\right)\kappa R_e \Psi_n'(\eta)\Psi_n(\eta) - 4\kappa^2\Psi_n'(\eta), \quad (34)$$

assume that the initial condition,

$$\Psi_o(\eta) = \sigma_1 + \sigma_2\eta + \sigma_3\frac{\eta^2}{2!}, \quad (35)$$

where,

$\Psi(0) = \sigma_1$, $\Psi'(0) = \sigma_2$, $\Psi''(0) = \sigma_3$,

from the boundary condition(29), we get

$$\Psi_o = 1 + \sigma_3\frac{\eta^2}{2}, \quad (36)$$

now, we have obtained a preliminary condition for solving the problem that contains σ_3 is unknown. we can obtain the value of σ_3 from the analytical approximate solution of Equation (34) at $\eta = 1$. The analytical approximate solutions of the Equation (28) in the following equations:

$$\Psi_1 = 1 + \left[\frac{1}{2}\sigma_3 - \frac{1}{120}\left(\frac{\beta}{1+\beta}\right)R_e\,\kappa\,{\sigma^2}_3\right]\eta^2 - \frac{1}{12}\left(\frac{\beta}{\beta+1}R_e\kappa\sigma_3 + 2\kappa\,\sigma_3\right)\eta^4, \quad (37)$$

$$\Psi_2 = 1 + \frac{1}{2}\sigma_3\,\eta^2 - \left[\frac{1}{12}\left(\frac{\beta}{1+\beta}\right)R_e\kappa\,\sigma_3 + \frac{1}{6}\,\kappa^2\,\sigma_3\right]\eta^4 + [\frac{1}{45}\;\kappa^3\,\sigma_3 + \frac{1}{45}\left(\frac{\beta}{1+\beta}\right)R_e\kappa^3\,\sigma_3$$
$$-\frac{1}{120}\left(\frac{\beta}{1+\beta}\right)R_e\kappa\,{\sigma_3}^2 + \frac{1}{180}\left(\frac{\beta}{1+\beta}\right)^2{R_e}^2\kappa^2\,\sigma_3]\,\eta^6 + [\frac{1}{280}\left(\frac{\beta}{1+\beta}\right)R_e\kappa^3\,{\sigma_3}^2 +$$
$$\frac{1}{560}\left(\frac{\beta}{1+\beta}\right)^2{R_e}^2\kappa^2\,{\sigma_3}^2\,]\,\eta^8 - [\frac{1}{3240}\left(\frac{\beta}{1+\beta}\right)R_e\kappa^5\,{\sigma_3}^2 - \frac{1}{3240}\left(\frac{\beta}{1+\beta}\right)^2{R_e}^2\kappa^4\,{\sigma_3}^2$$
$$+\frac{1}{10800}\left(\frac{\beta}{1+\beta}\right)^2{R_e}^2\kappa^2\,{\sigma_3}^3 + \frac{1}{12960}\left(\frac{\beta}{1+\beta}\right)^3{R_e}^3\kappa^3\,{\sigma_3}^3\,]\eta^{10} - [\frac{1}{47520}\left(\frac{\beta}{1+\beta}\right)^2{R_e}^2\kappa^4\,{\sigma_3}^3$$

$$+\frac{1}{95040}\left(\frac{\beta}{1+\beta}\right)^3 R_e{}^3\kappa^3\,\sigma_3{}^3]\,\eta^{12}-\left[\frac{1}{2620800}\left(\frac{\beta}{1+\beta}\right)^3 R_e{}^3\kappa^3\,\sigma_3{}^4\right]\eta^{14}. \quad (38)$$

$$\vdots$$

5. Results and Discussions.

In this section, the objective of the present study is to introduce the results of simulation for velocity from application P IA to obtain an analytical approximate solution of Jeffery Hamel flow fluid. Moreover, we discuss the effect of numerous emerging parameters as Casson fluid parameter β, Reynolds number R_e, and open angle κ on the velocity profile $\Psi(\eta)$. Testing the convergence of values of constants σ_3 is tabulated in Tables (5)- (8) for both diverging and converging which can be extracted from the boundary condition $\Psi(1)=0$. It can be shown that values of $\sigma_3$are convergent and being fixed in the fourth order of approximation. Effects of different parameters on the coefficient of skin friction are given in Table (9). This table displays comparison between the results presented and VPM, we can note that the solutions are well matched. As wall the magnitude of the skin friction coefficient decreases with an increase in R_e, β, and κ for diverging channel. For converging channel, the magnitude of the skin friction coefficient increases with an increase in R_e and κ while a decrease in the magnitude of the skin friction coefficient is found with an increase in β. In Tables (10) - (13), the values of velocity profile $\Psi(\eta)$ in the domain for some values of η are computed for different values of parameters. A comparison findings in which an outstanding consensus is excellent agreement between the solutions for both converging and diverging channels, are seen in theses Tables. Graphically, the influences of various parameters on the velocity $\Psi(\eta)$are plotted in Figures (2) and (3). The important effects of the present work are displays in two cases as follows:

- **Diverging channel.**

Figures (2a) - (2c) are showing effects of channel angle κ, Reynolds number R_e and Casson fluid parameter β respectively. for all these parameters, we have an almost equal effect on the velocity profile $\Psi(\eta)$. That is, the velocity profile decreased by changes in κ, R_e and β. The maximal velocity near the middle of the channel is found. It is important to note that β gives a basic Newtonian fluid velocity.

- **Converging channel.**

The results of the same parameters are depicted in Figures (3a) - (3c) for the converging

channel. In this case, a very opposite behavior is observed in the velocity $\Psi(\eta)$ for κ, R_e, and β. The effect of β is more significant in comparison with κ, R_e.

Table 5: The convergence of the values σ_3 for $\mathrm{R_e} = 100$, $\beta = 0.3$.

Approximation Order	σ_3	σ_3
η	$\kappa = 5^o$	$\kappa = -5^o$
1	-2.662059	-1.561842
2	-2.615389	-1.533696
3	-2.617581	-1.532479
4	-2.617523	-1.532444
5	-2.617524	-1.532444
6	-2.617524	-1.532444
7	-2.617524	-1.532444
8	-2.617524	-1.532444

Table 6: The convergence of the values σ_3 for $\mathrm{R_e} = 50$, $\beta = 0.4$.

Approximation Order	σ_3	σ_3
η	$\kappa = 2^o$	$\kappa = -2^o$
1	-2.14062317	-1.87424934
2	-2.13810451	-1.87208670
3	-2.13812208	-1.87206348
4	-2.13813201	-1.87206332
5	-2.13813201	-1.87206332
6	-2.13813201	-1.87206332
7	-2.13813201	-1.87206332
8	-2.13813201	-1.87206332

Table 7: The convergence of the values σ_3 for $R_e = 30$, $\beta = 0.5$

Approximation Order	σ_3	σ_3
η	$\kappa = 1^o$	$\kappa = -1^o$
1	-2.0475490960	-1.9544798460
2	-2.0472531070	-1.9542024530
3	-2.0472542390	-1.9542014070
4	-2.0472542360	-1.9542014050
5	-2.0472542360	-1.9542014050
6	-2.0472542360	-1.9542014050
7	-2.0472542360	-1.9542014050
8	-2.0472542360	-1.9542014050

Table 8: The convergence of the values σ_3 for $R_e = 10$, $\beta = 0.5$.

Approximation Order	σ_3	σ_3
η	$\kappa = 3^o$	$\kappa = -3^o$
1	-2.0344764290	-1.9699579320
2	-2.0343157880	-1.9698413420
3	-2.0343162420	-1.9698410590
4	-2.0343162410	-1.9698410590
5	-2.0343162410	-1.9698410590
6	-2.0343162410	-1.9698410590
7	-2.0343162410	-1.9698410590
8	-2.0343162410	-1.9698410590

Table 9: The values of skin friction coefficient $\left(1+\frac{1}{\beta}\right)\Psi'(1)$ for various parameters.

ω	R_e	β	λ_3	$R_e C_\Psi[15]$	$R_e C_\Psi$
1°	50	0.3	-2.054587195	-8.491011	-8.4911010
3°	50	0.3	-2.169422542	-8.132965	-8.1332390
5°	50	0.3	-2.292240285	-7.765948	-7.7663980
-1°	50	0.3	-1.947216335	-8.840078	-8.8399900
-3°	50	0.3	-1.846819550	-9.180186	-9.1799280
-5°	50	0.3	-1.752933827	-9.511377	-9.5109470
5°	100	0.3	-2.617581485	-6.879197	-6.8798250
5°	150	0.3	-2.983901230	-5.989193	-5.9892090
5°	200	0.3	-3.393374625	-5.101456	-5.0994860
-5°	100	0.3	-1.454410963	-10.363046	-10.709501
-5°	150	0.3	-1.340394520	-11.197414	-11.194771
-5°	200	0.3	-1.173470012	-12.012961	-12.006979
5°	50	0.1	-2.113842436	-21.068544	-21.069045
5°	50	0.5	-2.431945228	-5.1040820	-5.1044890
5°	50	0.9	-2.635817684	-3.3286000	-3.3289020
-5°	50	0.1	-1.901752215	-22.814960	-22.814574
-5°	50	0.5	-1.651240676	-6.8482430	-6.8477740
-5°	50	0.9	-1.5216913980	-5.0702750	-5.0697080

Table 10: Comparsion between PIA and VPM for $R_e = 100,\ \kappa = 5^0,\ \beta = 0.3$.

	VPM[15]	PIA	VPM[15]	PIA
η	For Diverging Channel		For Converging Channel	
0.0	1.000000	1.000000	1.000000	1.000000
0.1	0.986954	0.986959	0.986956	0.992313
0.2	0.948339	0.948346	0.968947	0.968943
0.3	0.885656	0.885670	0.928987	0.928978
0.4	0.801219	0.801240	0.870919	0.870905
0.5	0.697894	0.697923	0.792662	0.792643
0.6	0.578809	0.578842	0.691628	0.691604
0.7	0.447036	0.447070	0.564845	0.564819
0.8	0.305319	0.305348	0.409171	0.409148
0.9	0.155833	0.155851	0.221645	0.221629
1.0	0.000000	0.000000	0.000000	0.000000

Table 11:Comparsion between PIA and RK4 for $R_e = 50,\ \kappa = 2^0,\ \beta = 0.4$.

	PIA	RK4	PIA	RK4
η	For Diverging Channel		For Converging Channel	
0.0	1.000000	1.000000	1.000000	1.000000
0.1	0.989318	0.989318	0.990631	0.990631
0.2	0.957378	0.957378	0.962435	0.962435
0.3	0.904491	0.904491	0.915139	0.915139
0.4	0.831145	0.831145	0.848304	0.848304
0.5	0.737975	0.737975	0.761349	0.761349
0.6	0.625710	0.625710	0.653585	0.653585
0.7	0.495111	0.495111	0.524262	0.524262
0.8	0.346909	0.346909	0.372634	0.372634
0.9	0.181726	0.181726	0.198039	0.198039
1.0	0.000000	0.000000	0.000000	0.000000

Table 12 :Comparison between PIA and RK4 for $R_e = 30$, $\kappa = 1^0$, $\beta = 0.5$.

	PIA	RK4	PIA	RK4
η	For Diverging Channel		For Converging Channel	
0.0	1.000000	1.000000	1.000000	1.000000
0.1	0.989766	0.989766	0.990226	0.990226
0.2	0.959102	0.959102	0.960871	0.960871
0.3	0.908110	0.908110	0.911835	0.911835
0.4	0.836957	0.836957	0.842960	0.842960
0.5	0.745860	0.745860	0.754037	0.754037
0.6	0.635067	0.635067	0.644821	0.644821
0.7	0.504847	0.504847	0.515049	0.515049
0.8	0.355458	0.355458	0.364461	0.364461
0.9	0.187122	0.187122	0.192832	0.192832
1.0	0.000000	0.000000	0.000000	0.000000

Table 13 :Comparison between PIA and RK4 for $R_e = 10$, $\kappa = 6^0$, $\beta = 0.4$.

	PIA	RK4	PIA	RK4
η	For Diverging Channel		For Converging Channel	
0.0	1.000000	1.000000	1.000000	1.000000
0.1	0.989560	0.989560	0.990351	0.990351
0.2	0.958309	0.958309	0.961353	0.961353
0.3	0.906441	0.906441	0.912849	0.912849
0.4	0.834266	0.834266	0.844591	0.844591
0.5	0.742188	0.742188	0.756250	0.756250
0.6	0.630680	0.630680	0.647446	0.647446
0.7	0.500245	0.500245	0.517773	0.517773
0.8	0.351377	0.351377	0.366840	0.366840
0.9	0.184517	0.184517	0.194318	0.194318
1.0	0.000000	0.000000	0.000000	0.000000

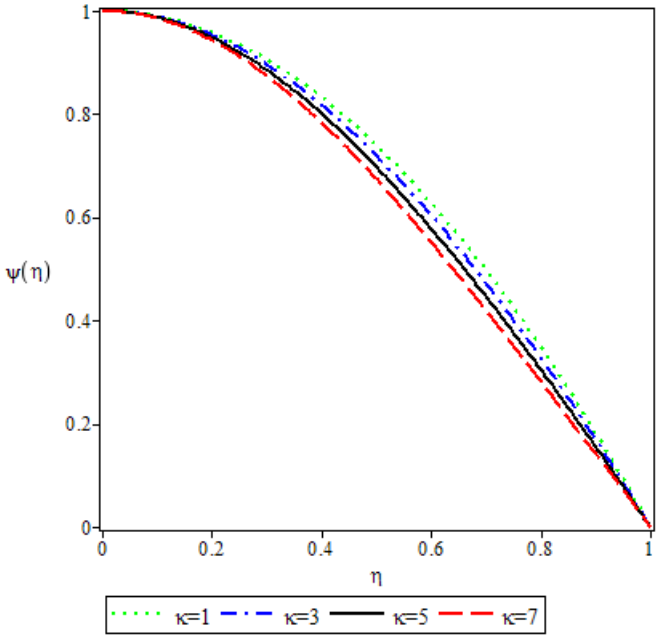

(a) $\beta = 0.3$, $R_e = 100$

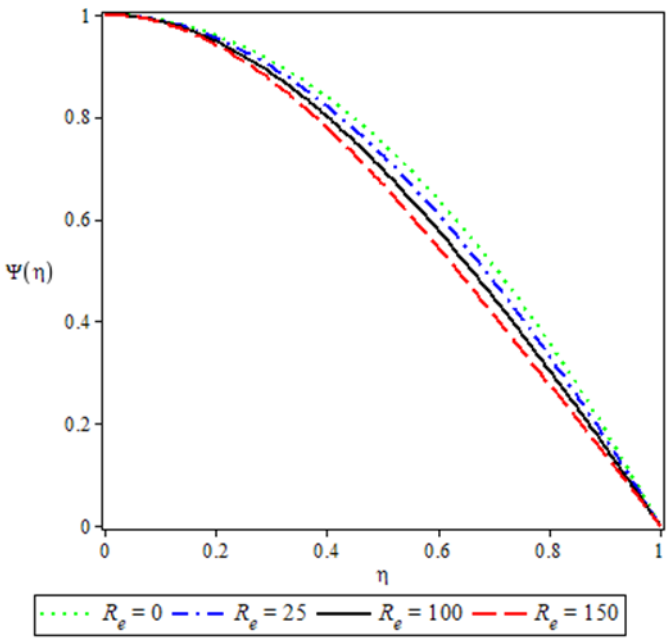

(b) $\beta = 0.3$, $\kappa = 5^{\circ}$

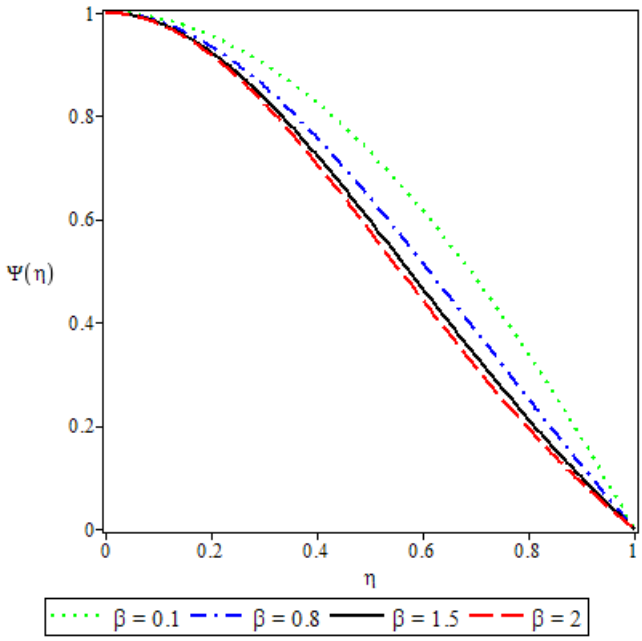

(c) $R_e = 100$, $\kappa = 5^{\circ}$

Figure 2: The curves of the $\Psi(\eta)$ (a) several values of κ, (b) several values of R_e and (c) several values of β.

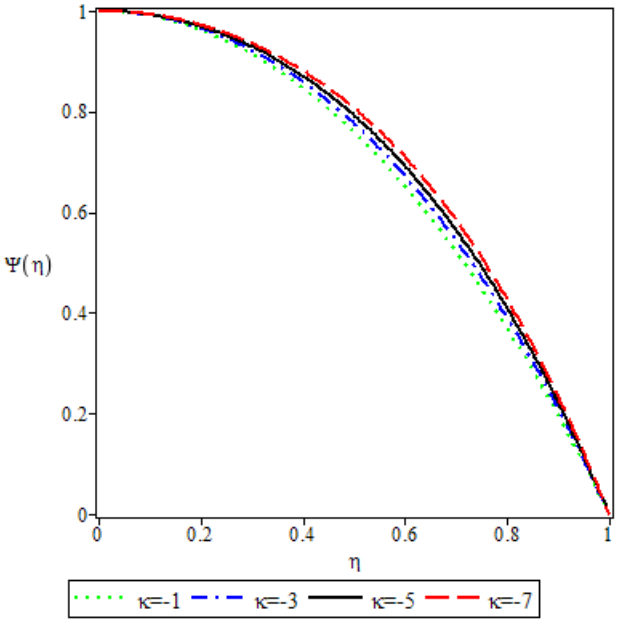

$(a)\ \beta = 0.3,\ R_e = 100$

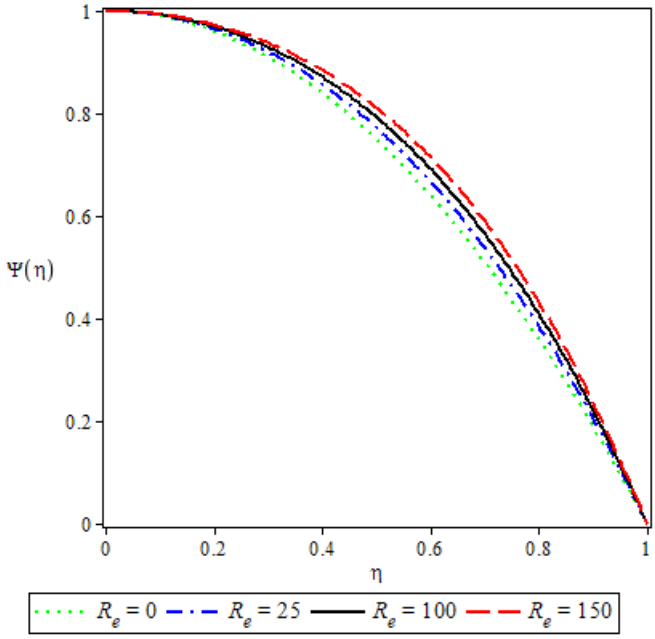

$(b)\ \beta = 0.3,\ \kappa = -5$

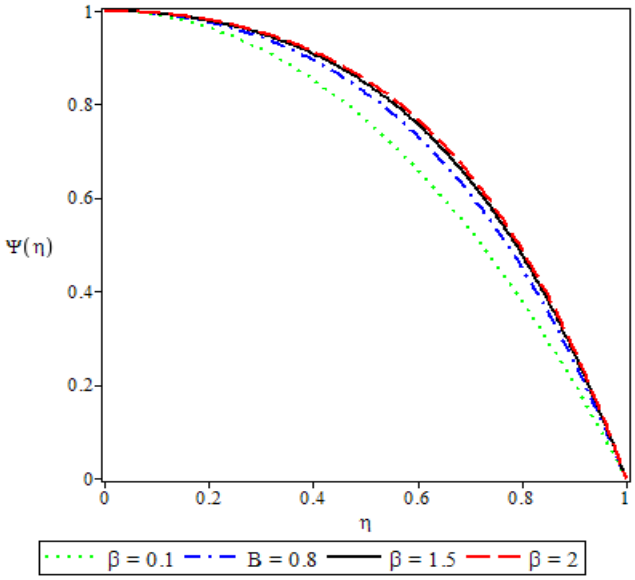

$(c)\ R_e = 100,\ \kappa = -5^{\circ}$

Figure 3: The curves of the $\Psi(\eta)$ (a) several values of κ, (b) several values of R_e and (c) several values of β.

Conclusions

Non-Newtonian Jeffery Hamel flow of Casson fluid problem is presented and solved using PIA technique. The figures that presented to study the behavior of emerging physical parameters showed an increase in values of parameters and the behavior of the velocity in the widening channel is opposite to in the narrowing channel. In general, similarity transformation is an important role to transform the non-linear partial differential equations of Jeffery Hamel fluid flow problems for all data into non-linear ordinary differential equations with boundary conditions that found are easy to solve by PIA. Finally, the numerical values for skin friction for varying Reynolds number, Casson fluid parameter, and open angle are discussed.

References

[1] GB. Jeffery, The two-dimensional steady motion of a viscous fluid, Philos. Mag., 29(1915) 455-465

[2] G. Hamel, Spiralformige bewegungen zaher flussigkeiten, Math. Verein., 25(1916)34-60

[3] Wl. Axford, The magnetohydrodynamics Jeffery-Hamel problem for a weakly conducting fluid, Q. J. Mech. Appl. Math., 14(1961)335-351

[4] Z.Ganji, D.D. Ganji, and M. Esmaeilpour, Study on nonlinear Jeffery-Hamel flow by Hes semi-analytical methods and comparison with numerical results, Comp. Math. Appl., 58 (2009) 2107-2116

[5] S. Alao, E.I. Akinola, K.A. Salaudeen, R.A. Oderinu, and F.O. Akinpelu, On the solution of MHD Jeffery-Hamel flow by weighted residual method, Int. J. Chem.,1 (2017) 80-85

[6] A. A. Joneidi, G. Domairry, and M. Babaelahi, Three analytical methods applied to Jeffery-Hamel flow, Comp. Nonlin. Sci. Numer. Sim., 15(2010) 3423-3434

[7] U. Khan, N. Ahmed, and S. T. Mohyud-Din, Soret and Dufour effects on flow in converging and diverging channels with chemical reaction, Aerosp. Sci. Technol., 49 (2016)135-143

[8] D. A. McDonald, Blood Flows in Arteries, 2nd ed., Arnold, London (1974)

[9] Q. Esmaili, A. Ramiar, E. Alizadeh, and D.D. Ganji, An approximation of the analytical solution of the Jeffery-Hamel flow by decomposition method, Phys. Let. A., 372 (2008) 3434-3439

[10] S. Nadeem, R.U. Haq, C. Lee, MHD flow of a Casson fluid over an exponentially shrinking sheet, Sci. Iran., 19 (2012) 1150-1553

[11] M. Asadullah, U. Khan, R. Manzoor, N. Ahmed, S. T. Mohyud-din, MHD flow of a Jeffery fluid in converging and diverging channels, Int. J. Mod. Math. Sci., 6(2013)92-106

[13] S. Motsa, P.Sibanda, F. Awad, and S. Shateyi, A new spectral-homotopy analysis method for the MHD Jeffery-Hamel problem, Comp. Fluids, 39(2010)1219-1225

[14] S. Moghimi, G. Domairry, S. Soleimani, E. Ghasem, and G. Bararnia, Application of homotopy analysis method to solve MHD Jeffery-Hamel flows in nonparallel walls, Adv. Eng Softw., 42(2011)108-113

[15] U. Khan1 , N. Ahmed , W. Sikandar , S. T. Mohyud-Din, Jeffery Hamel flow of a non-newtonian fluid, J. Appl. Comp. Mech., 2(2016) 21-28

[16] A. J. Harfash A. J. Al-Saif, MHD Flow of Fourth Grade Fluid Solve by Perturbation Iteration Algorithm, J. Adv. Res. Fluid Mech. Therm. Sci., 59 (2020) 220-231

[17] A. J. A. Al-Saif, and A. M. Jasim, A novel algorithm for studying the effects of squeezing flow of a Casson Fluid between parallel plates on magnetic field, J. of Appl. Math.,(2019).

[18] A. J. A. Al-Saif, and A. M. Jasim, New Analytical Study of the Effects Thermo- Diffusion, Diffusion-Thermo and Chemical Reaction of Viscous Fluid on Magneto Hydrodynamics Flow in Divergent and Convergent Channels, Appl. Math., 10(2019) 268-300.

[19] A. J. A. Al-Saif, and A. M. Jasim, Analytical Investigation of the MHD Jeffery-Hamel Flow Through Convergent and Divergent Channel by New Scheme, Eng. Let., 27(2019)1-28.

[20] A. M. Jasim, A. J. A. Al-Saif,New Analytical Solution Formula for Heat Transfer of Unsteady Two-Dimensional Squeezing Flow of a Casson Fluid between Parallel Circular Plates, J. Adv. Res. Fluid Mech. Therm. Sci., 2(2019) 219-243

[21] A. M. Jasim, Analytical approximation of the first grade MHD squeezing fluid flow with slip boundary condition using a new iterative method, Heat Transf., (2020)1-21

[22] A. M. Jasim, New analytical study for nanofluid between two non-parallel plane palls (Jeffery-Hamel Flow), J. Appl. Comp. Mech., 7 (2021) 213-224

[23] A. J. Al-Saif, A. J. Harfash, Perturbation-Iteration Algorithm for Solving Heat and Mass Transfer in the Unsteady Squeezing Flow between Parallel Plates, J. Appl. Comp. Mech., 5(2019) 804-815

[24] N. B. DIK, General Convergence Analysis for the Perturbation Iteration Technique, Turk. J. Math. Comp. Sci., 6(2017)1- 19

دراسة تحليلية جديدة لتدفق جيفري هامل لا نيوتوني لمائع كاسون في القناة المتقاربة والمتباعدة بواسطة خوارزمية الاضطراب التكراري

عبير مجيد جاسم ، علي جويعد المالكي

المستخلص

في هذه المقالة ، يتم استخدام خوارزمية تكرار الاضطراب لحل مسا ئلة تدفق جيفري هامل للسائل غير النيوتوني وهو سائل كاسون للتبسيط ، يتم تطبيق تحويل مناسب لأوجه التشابه للحصول على معادلة التفاضلية الغير خطية العادية. يتم حل المعادلة الناتجة عن طريق خوارزمية تكرار الاظطراب وعدديًا باستخدام رنجا كتامن الدرجة الرابعة تتم مقارنة كلا الحلين مع تباين تقنية المعلمات من أجل التحقق من فعالية النهج بشرط لكل من القنوات المتباعدة والمتقاربة ، يتم توضيح تأثيرات المعلمات باستخدام المحاكاة الرسومية